

Received November 6, 2020, accepted December 2, 2020, date of publication December 21, 2020, date of current version December 31, 2020.

Digital Object Identifier 10.1109/ACCESS.2020.3046088

Impulsive Flashover Characteristics and Weibull Statistical Analysis of Gas-Solid Interfaces With Varying Relative Humidity

RUAIRIDH W. MACPHERSON¹, (Graduate Student Member, IEEE),
MARK P. WILSON¹, (Member, IEEE), **IGOR V. TIMOSHKIN**¹, (Senior Member, IEEE),
SCOTT J. MACGREGOR¹, (Senior Member, IEEE),
AND MARTIN J. GIVEN¹, (Senior Member, IEEE)

Department of Electronic and Electrical Engineering, University of Strathclyde, Glasgow G1 1XW, U.K.

Corresponding author: Ruairidh W. Macpherson (ruairidh.macpherson@strath.ac.uk)

The work of Ruairidh W. Macpherson was supported in part by the EPSRC under Grant EP/N509760/1.

ABSTRACT This paper informs on the flashover strength of three materials: Delrin (polyoxymethylene), HDPE (high-density polyethylene) and Ultem (polyetherimide) with smooth surface finishes, in zero-grade air at -0.5 , 0 and 0.5 bar gauge, and at $<10\%$, $\sim 50\%$ and $>90\%$ relative humidity (RH). Both negative and positive polarity impulse voltages were applied to investigate the potentially asymmetrical electrical performance of the geometrically-symmetrical electrode arrangement. In all tests, high voltage (HV) impulses with a nominal $100/700$ ns wave-shape were applied. Each test conformed with the ASTM D3426-97 standard of 'step up' testing, to find the average flashover voltage for each set of conditions. For negative polarity, each solid dielectric material demonstrated a decrease in flashover voltage as the RH was increased. For positive polarity, however, the flashover voltages were similar for all levels of RH, with the exemption of HDPE. A decrease in flashover voltage was found as the permittivity of the material increased for negative polarity, irrespective of humidity and pressure. Overall, the highest flashover voltage recorded for negative polarity was ~ 200 kV with an HDPE spacer, at 0.5 bar gauge and $<10\%$ RH. The poorest performance was for a Delrin spacer in negative polarity, at -0.5 bar gauge and $>90\%$ RH, at a value of ~ 53 kV. For positive polarity, the highest flashover voltage was for a Delrin spacer at $\sim 50\%$ RH and 0.5 bar gauge, with a voltage of ~ 180 kV; the lowest flashover voltage of ~ 60 kV was recorded with an HDPE spacer, at -0.5 bar gauge and $>90\%$ RH.

INDEX TERMS Flashover, gas breakdown, high-density polyethylene, high voltage, impulse, polyetherimide, polyoxymethylene, pulsed power, relative humidity, surface flashover, Weibull statistical analysis, zero-grade air.

I. INTRODUCTION

Solid insulation is important within pulsed power systems as it provides mechanical support between conductors at different potential, but the inclusion can lead to surface flashover of the gas-solid interface created, which can occur at a lower applied voltage than that for a gas gap without a solid spacer. Therefore, it is desirable to have information on the flashover strength of different materials within a system, in order for design processes to be tailored to the intended application. Within this paper, solid spacers were tested in sub-optimal conditions, and the performance recorded throughout. Three

materials, HDPE (high-density polyethylene), Delrin (polyoxymethylene) and Ultem (polyetherimide) were tested in conditions of varying humidity, polarity and pressure.

Experimental results are reported in [1], with surface flashover events characterised in air with varying humidity for PTFE, silicone rubber (SIR), nylon and glazed porcelain, with a rod-plane electrode topology, under positive impulse voltages. The authors observed that, as the absolute humidity increased from 5 g/m^3 to 25 g/m^3 , the positive flashover voltage was seen to increase for both lightning impulse (LI) and switching impulse (SI) voltages.

In [2], under a similar topology and negative polarity, it was observed that increasing the relative humidity (RH) resulted in the flashover strength decreasing. The flashover voltage

The associate editor coordinating the review of this manuscript and approving it for publication was Mehdi Bagheri¹.

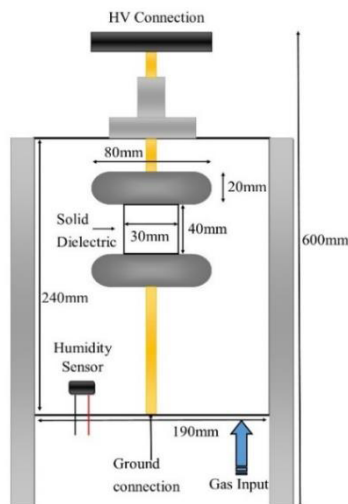


FIGURE 1. Schematic diagram of test cell, showing spacer between electrodes, dimensions and connections.

was recorded at 10%, 30%, 60% and 90% RH, and decreased from 18 kV to 14 kV. In [3], the differences in the initiation and propagation of positive and negative streamers, resulting in flashover, are discussed. It was found that, under negative polarity, the plasma channel established at breakdown was seen to follow the surface of the material. Under positive polarity, however, the plasma channel at breakdown was seen to be repelled from the surface of the solid material and propagate through the bulk air.

In [4], flashover of air gaps without solid spacers was characterised, under high humidity levels, up to and including 100% RH. Under these conditions, fog accumulation was found to have a detrimental effect on the breakdown strength of the air gap tested, especially for values of RH > 80%.

In [5], the effect of increasing water vapour content in SF₆ was investigated. The authors found that the increase of water content at a given pressure resulted in a decrease in the flashover strength of an epoxy-resin insulated system. It was also found that the presence of water for an extended period of time could result in chemical reactions occurring at the spacer surface, leading to reduced flashover initiation voltages.

Within the present work, three different humidity levels were used throughout the testing process: <10% RH, ~50% RH and >90% RH. Flashover under both, positive and negative, polarity impulse voltages was investigated, at pressures of -0.5 bar gauge, 0 bar gauge and 0.5 bar gauge. Previous literature reports on the performance of various different materials in high-humidity environments show different behaviour under similar conditions [1]–[4]. The materials tested in this paper were HDPE (high-density polyethylene), Ultem (polyetherimide) and Delrin (polyoxymethylene). The relative permittivity of these materials is 2.3 [6], 3.0 [7] and 3.8 [8], respectively. The dimensions of the solids used were 40 mm in length and 30 mm in diameter, as shown in Fig. 1.

This paper focuses on similar methodology to that used in the literature discussed previously, although under the

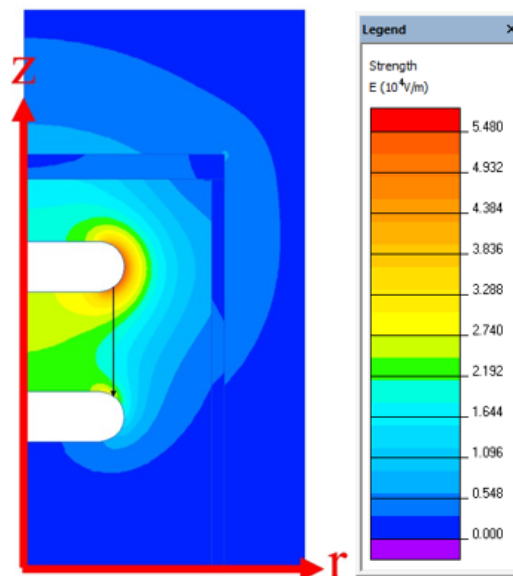


FIGURE 2. Asymmetric electric field distribution for test cell setup, with boundary conditions added to simulate the practical position within the Faraday-caged lab; 1 kV is applied to the upper electrode and the lower electrode is grounded. Materials for the test cell enclosure shown in the figure are PVC on the top and bottom of the test cell and Perspex for the enclosure, corresponding to Figure 1. Boundary conditions (not shown due to the long distances involved) are at 1.5 m from the electrode edges to the side wall of the lab (*r* direction), and at 1.25 m from the electrodes to the lab ceiling (*z* direction), which correspond to the physical distances in the test lab.

high dV/dt conditions encountered in pulsed power applications, in order to determine the effect of environmental conditions on the relative flashover performance of the different solid materials, thereby, allowing conclusions to be drawn on the synergistic effect of multiple environmental and material parameters on the flashover voltage. This paper also highlights the potential asymmetrical electrical behaviour of geometrically-symmetrical electrode arrangements, due to the ratio of the sparkover distance to the electrode diameter. The reported results, highlighting the effect of sub-optimal conditions on the fast dV/dt impulsive flashover of solid insulation, will be of interest to designers of high voltage and pulsed power components and systems.

II. EXPERIMENTAL ARRANGMENT

In Fig. 1, the design of the test cell has been illustrated, including the dimensions of each component part. The arrangement was designed in order to replicate a practical pulsed power insulation system, where limited space is available. The electrodes shown are made of stainless-steel and polished to a mirror finish. The specific shape of the electrodes resulted in a quasi-uniform electrical field distribution being produced during energization. From an axisymmetric electrostatic simulation run using QuickField software, an increase in the field intensity of ~87% at the rounded edges of the electrodes was measured, in comparison to the average field (V/d), as shown in Fig. 2. The simulation result in Fig. 2, which was conducted

for an open gap with no solid spacer, also shows that the electric field strength is 103% higher at the HV electrode in comparison to that at the grounded electrode, over the contour line shown. The simulations were focused on open gaps, to highlight the possibility of differences in positive and negative breakdown voltages, even in the geometrically-symmetrical electrode arrangement, when one electrode is grounded. The simulation incorporates the Laplacian equation: $\nabla^2 V = 0$, and a Dirichlet boundary condition of $V = 0$ was used to simulate the effects of measured distances to grounded parts of the Faraday test cage where the test cell was housed. This resulted in an asymmetric electric field distribution, prompting both impulse polarities to be tested.

The system was designed to limit the maximum breakdown voltage to around 200 kV. These design criteria resulted in asymmetrical electrical behaviour of the geometrically-symmetrical electrode arrangement, including in the case when the electrodes were not bridged by a solid spacer. For such open air gaps, this behaviour is due to the ratio of the inter-electrode gap spacing and the diameter of the electrodes, as shown in [9], and discussed further in [10]. Based upon the discharge regimes discussed in [9] and [10], the dimensions of the electrode system used herein, where the discharges generally occur at the rounded edges of the electrodes for no-spacer tests, fall within the ‘low positive spark over range’ from [10], due to the ratio of the diameter of the electrode edge (20 mm) to gap distance (40 mm) being 200%; this is discussed further in section V.

This ratio results in a lower positive breakdown voltage than negative, for geometrically-symmetrical electrode arrangements, when one of the electrodes is grounded [9]. Therefore, both positive- and negative-polarity impulse voltages were applied in the present work, to establish whether a similar effect was observed.

The charging voltage was supplied from a 100 kV, 2.5 mA, Glassman high voltage DC power supply, connected through a 1 M Ω charging resistor. This was then connected to the input of a 10-stage Marx generator. The CuSO₄ wave-shaping resistors used had values of 300 Ω for the wave-tail and 700 Ω for the output (wave-front) resistor, as illustrated in Fig. 3. This specific resistor arrangement resulted in a 100/700 ns output voltage waveform, as shown in the oscillograms in Fig. 4. The output of the Marx generator was connected to the test cell and a voltage divider in parallel. A 1000:1 Tektronix P6015A HV probe was connected to the output of an 8:1 CuSO₄ resistive voltage divider, and through to a Tektronix MDO3012 oscilloscope, for analysis of the resulting waveforms.

Several stages were incorporated into the gas-handling system, allowing for the relative humidity of the gas in the test cell to be altered and monitored prior to testing. This was achieved using a ‘wet chamber’, connected to a gas distribution board, where air could be passed through a chamber filled with distilled water and an ultrasonic humidifier, before entering the test cell. The output of the gas bottle was connected to both, a ‘dry line’ and a ‘wet line’, allowing

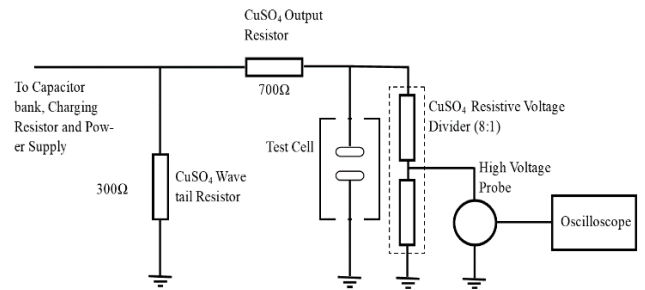


FIGURE 3. Circuit diagram of components connected to the output of the Marx generator, with resistor values used to produce the 100/700 ns waveshape.

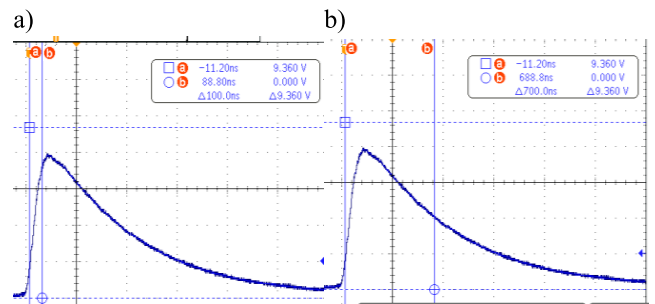


FIGURE 4. Resulting positive polarity waveform from Marx generator, showing a) Rise time of 100 ns (10% - 90%) and b) Time to half-value of 700 ns.

for <10%, ~50% and >90% RH to be achieved. Dry air with <10% RH was provided directly from the gas bottle; the test-cell was evacuated 3 times using a rotary vacuum pump before testing to remove any residual humidity, before finally filling with the gas to be tested. Relative humidity of ~50% was achieved by mixing gas from the gas bottle line, which bypasses the wet chamber, and a line that flows through the wet chamber. Relative humidity of >90% was achieved by passing gas only through the wet chamber. The achieved humidity was then monitored by a TE Connectivity HPP801A031 humidity sensor, the output capacitance of which varies with RH ($\pm 2\%$), housed within the test cell, as shown in Fig. 1. The sensor was connected via a buffer circuit, with changes in the frequency of the output signal corresponding to changes in RH, to a separate Rohde and Schwarz HMO2024 oscilloscope, allowing the humidity to be monitored throughout the testing process. The test cell chamber was re-filled each time a flashover event occurred, after being evacuated using the rotary vacuum pump. The vacuum pump was also used in controlling and setting the internal test cell pressure, prior to testing.

The testing procedure implemented was a ‘step up’ method, as included in the ASTM D3426-97 standard [11]. The voltage level initially applied was set to provide a low probability of flashover, before the charging voltage was increased in iterations of 300 V, monitored on a DMM, via a 1000:1 Testec HVP-40 HV probe. Once a flashover event was initiated during one of the three tests at each level,

the resulting waveform was inspected, and the flashover voltage recorded. The output voltage was then decreased to a level with a low probability of breakdown, and the process repeated until the occurrence of another flashover event. Two, clear, withstand levels were always observed before a valid breakdown voltage was recorded. This process was conducted $N = 20$ times for each set of test conditions. The obtained breakdown voltage values, U_i , were used to obtain an estimation of the flashover initiation voltage, U_{50} , as shown in (1).

$$U_{50} = \sum_{i=1}^N \frac{U_i}{N} \quad (1)$$

Fig. 3 shows a circuit diagram of the connections from the output of the Marx generator, connected to the test cell and the monitoring station where the data was recorded. Fig. 4 shows the resulting (positive) 100/700 ns output voltage waveform.

III. EXPERIMENTAL RESULTS

Figs. 5a (negative) and 6a (positive) show average flashover voltages at -0.5 bar gauge, Figs. 5b and 6b show results at 0 bar gauge, and Figs. 5c and 6c show results at 0.5 bar gauge. Each bar represents the average of 20 breakdown events, with the calculated standard deviation shown in the form of error bars.

Figs. 5a, 5b and 5c show the average flashover voltages and standard deviations calculated from the negative polarity data. It is clear that the flashover voltage of the insulation system generally decreased as the RH was increased. In all tests conducted, as the pressure was increased, the flashover voltage increased also. The maximum average flashover voltage of ~ 200 kV achieved in the tests was with an HDPE spacer under negative polarity, at 0.5 bar gauge and $<10\%$ RH. The minimum average flashover voltage of ~ 53 kV was recorded at -0.5 bar gauge and $>90\%$ RH, for a Delrin spacer. The effect of increasing RH can be seen for the 'Air' (no spacer) tests. A decrease in average flashover voltage was seen as the RH was increased, especially from $\sim 50\%$ to $>90\%$. At $>90\%$ RH, the test cell was in a fog-like environment, resulting in a significant decrease in the breakdown strength of the air gap, seen also in [4] and [12]. A permittivity effect on the flashover strength of the composite insulation system is also apparent in Figs. 5a, 5b and 5c, where a decrease in the flashover voltage was seen with increasing relative permittivity of the solid spacer; these decreases, however, are not statistically significant.

Figs. 6a, 6b and 6c show the positive polarity voltages for each material, humidity and pressure. There is a difference in insulation performance compared to the negative polarity results. Generally, at a particular pressure, the flashover strength of the system either stayed consistent, or increased slightly, from $<10\%$ RH to $\sim 50\%$ RH. With no spacer ('Air'), increasing humidity did not have a significant effect on the breakdown strength; this applied for all tested pressures, and was also observed in [13]. When a solid spacer was included,

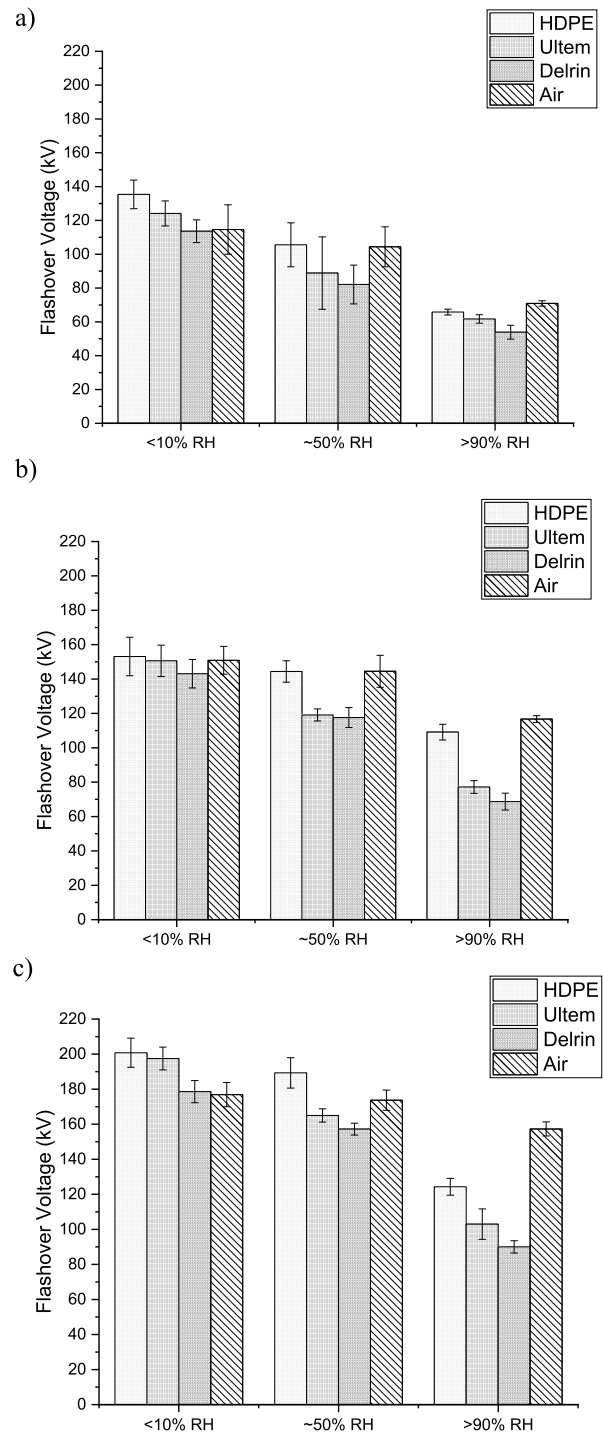


FIGURE 5. Negative polarity U_{50} flashover voltage results for HDPE, Ultem, Delrin and Air (no spacer), under $<10\%$ RH, $\sim 50\%$ RH and $>90\%$ RH, at: a) -0.5 bar gauge; b) 0 bar gauge; and c) 0.5 bar gauge. Each bar represents the average of 20 flashover events and the error bars show the standard deviation.

increasing relative permittivity did not result in the general trends seen during the negative polarity tests. The maximum achieved flashover voltage under positive polarity was found with a Delrin spacer, at $\sim 50\%$ RH and 0.5 bar gauge,

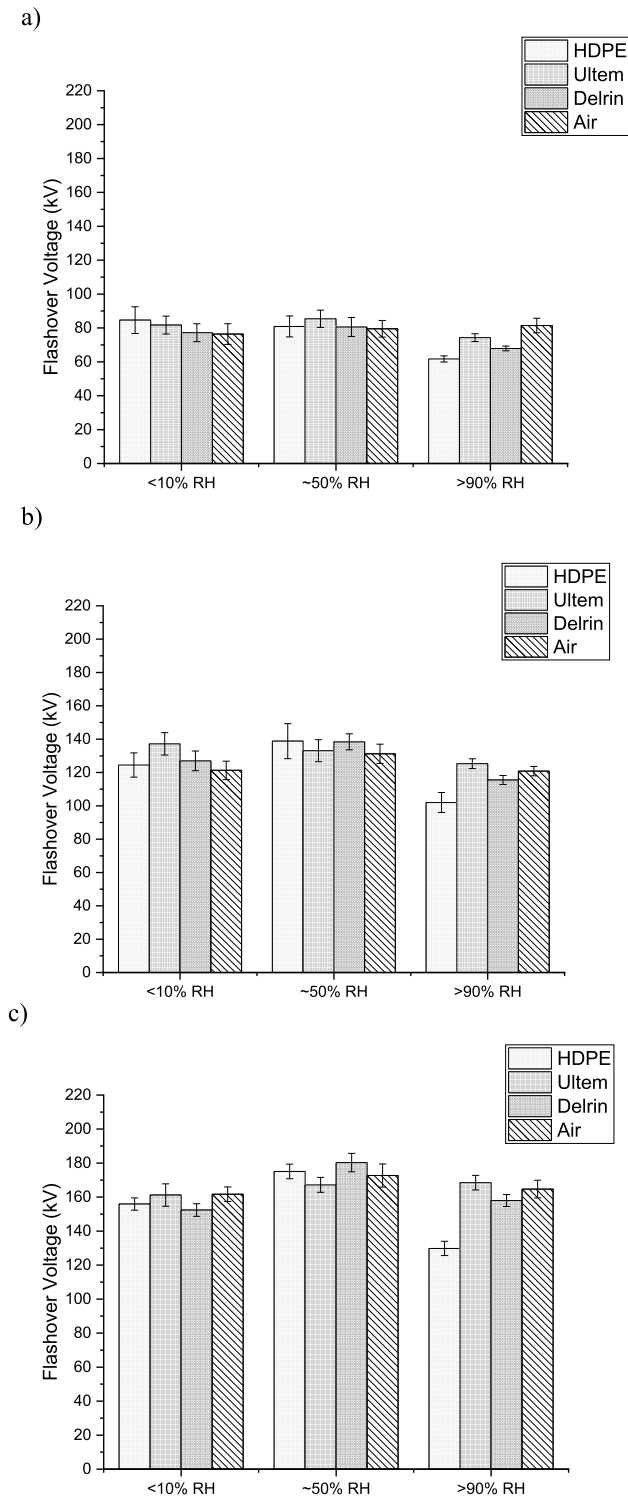


FIGURE 6. Positive polarity U_{50} flashover voltage results for HDPE, Ultem, Delrin and Air (no spacer), under <10% RH, ~50% RH and >90% RH, at: a) -0.5 bar gauge; b) 0 bar gauge; and c) 0.5 bar gauge. Each bar represents the average of 20 flashover events and the error bars show the standard deviation.

measured at a voltage of ~180 kV. The minimum flashover voltage of ~60 kV recorded under positive polarity was found at -0.5 bar gauge and >90% RH, with an HDPE spacer.

As the humidity increased, there was no conclusive difference in the flashover voltage, with the exception of HDPE, particularly at >90% RH; these results will be discussed further in section V, in the context of observations of differences in the discharge path for different conditions.

Comparison of results for both polarities shows a significant difference in the performance of the different materials during testing. For example, for an HDPE spacer at <10% RH and 0.5 bar gauge, the breakdown voltage fell from ~200 kV for negative polarity to ~155 kV for positive polarity. However, an increase in breakdown voltage, from ~90 kV for negative polarity to ~160 kV for positive polarity at >90% RH, was found for a Delrin spacer at 0.5 bar gauge. This asymmetrical behaviour is due to different phenomena governing the flashover process, discussed in section V.

When comparing negative and positive breakdown voltages at <10% RH, the differences between the voltages at each pressure are statistically significant to one standard deviation. This has been discussed in [9] and [10], where the specific electrode diameters and gap spacings result in a difference in the positive and negative breakdown voltages, for sphere-sphere gaps, with one electrode grounded. The dimensions used in the present study, displaying the asymmetric field distribution shown in Fig. 2 and using the same process as [9], [10], mean that the current electrode system can be categorised in the ‘low positive spark over range,’ resulting in a higher negative breakdown voltage. However, when adding moisture to the system, the breakdown voltages at ~50% RH and at >90% RH showed an increasingly-symmetrical performance, with the negative and positive breakdown voltages being closer in magnitude. This is potentially due to the effect on the field distribution of a build-up of moisture on the grounded electrode of the vertically-aligned electrode system, as well as its effect on the plasma channel location. This is discussed further in section V.

In order to illuminate the relative effects of the different experimental conditions further in section IV, a 2-parameter Weibull statistical analysis was conducted on the breakdown data for all different tests.

IV. 2-PARAMETER WEIBULL STATISTICAL ANALYSIS

A 2-parameter Weibull statistical analysis, which is often applied to insulation breakdown data, was performed on all breakdown results shown in Figs. 5 and 6. In this work, V is the peak applied voltage that was found to induce flashover [14]. Using the 2-parameter Weibull distribution (2) from [15], and introduced in [16], two parameters characterizing the distribution are found per data set.

$$F(V) = 1 - \exp\left[-\left(\frac{V}{\alpha}\right)^\beta\right] \quad (2)$$

The first parameter, α (kV), defines the offset voltage, V , where the probability of breakdown is 63.2%, $V_{63.2\%} = \alpha$. The second parameter, β , is used to control the skewness and the kurtosis of the distribution, and is found from the

gradient of the distribution. Lastly, the breakdown voltage associated with 0.01% probability of failure, $V_{0.01\%}$, was calculated from the cumulative distribution function (CDF) for each data set, in order to estimate the minimum breakdown (flashover) voltage for each test. To find each of these values, it was assumed that the voltage where the probability of failure of the insulation system is zero, γ , is $\gamma = 0$ V. A 3-parameter Weibull distribution fitting was also conducted for the test results. However, due to the computed γ values falling just below the minimum measured breakdown voltage values for each test, conservatively, the 2-parameter method was used, as well as finding the associated $V_{0.01\%}$ for each data set. This method was further validated in terms of goodness of fit by using a Kolmogorov-Smirnov test to 95% confidence level on each of the data sets.

Equation (2) characterises the cumulative probability of failure, and gives a distribution of flashover voltages with respect to probability of failure occurring. To form probability plots to compare the behavior of the different gas-solid (or gas only) gaps, the CDF from (2) is converted into the linear form shown in (3):

$$\ln \left[\ln \frac{1}{1 - F(V)} \right] = \beta \ln(V) - \beta \ln(\alpha) \quad (3)$$

Using (2) and (3), values for α and β were extracted from the results, and $V_{0.01\%}$ calculated. The values of α , β and $V_{0.01\%}$ for each of the tests are presented in Figs. 7 and 8.

A. WEIBULL DISTRIBUTION PARAMETERS

In this section, the Weibull parameters discussed previously have been graphed to show values of α , β and $V_{0.01\%}$.

1) NEGATIVE POLARITY

This section includes the 2-parameter Weibull analysis results corresponding to the negative-polarity flashover data in Fig. 5.

The parameters characterising the Weibull distributions for negative polarity results are shown in Figs. 7a (<10% RH), 7b (~50% RH) and 7c (>90% RH). For negative polarity, the 0.01% probability of failure value follows a similar trend to that of the α value. The difference between the α and 0.01% probability value is determined by the gradient (β) of the distribution, which is indicative of the sensitivity of the material tested. This can be seen visually in Fig. 7c, for example, where the 0.01% probability value is closer to the α value at -0.5 bar gauge, corresponding with the increasing values of β observed with decreasing permittivity. The values for 0.01% probability are reduced, in comparison to the α value, the most at -0.5 bar gauge and ~50% RH, from the lower β value measured due to the increased range of the breakdown voltages for these conditions, particularly for Ultem. The value of β was found to be fairly consistent with increasing pressure, although, the distribution becomes more erratic at >90% RH.

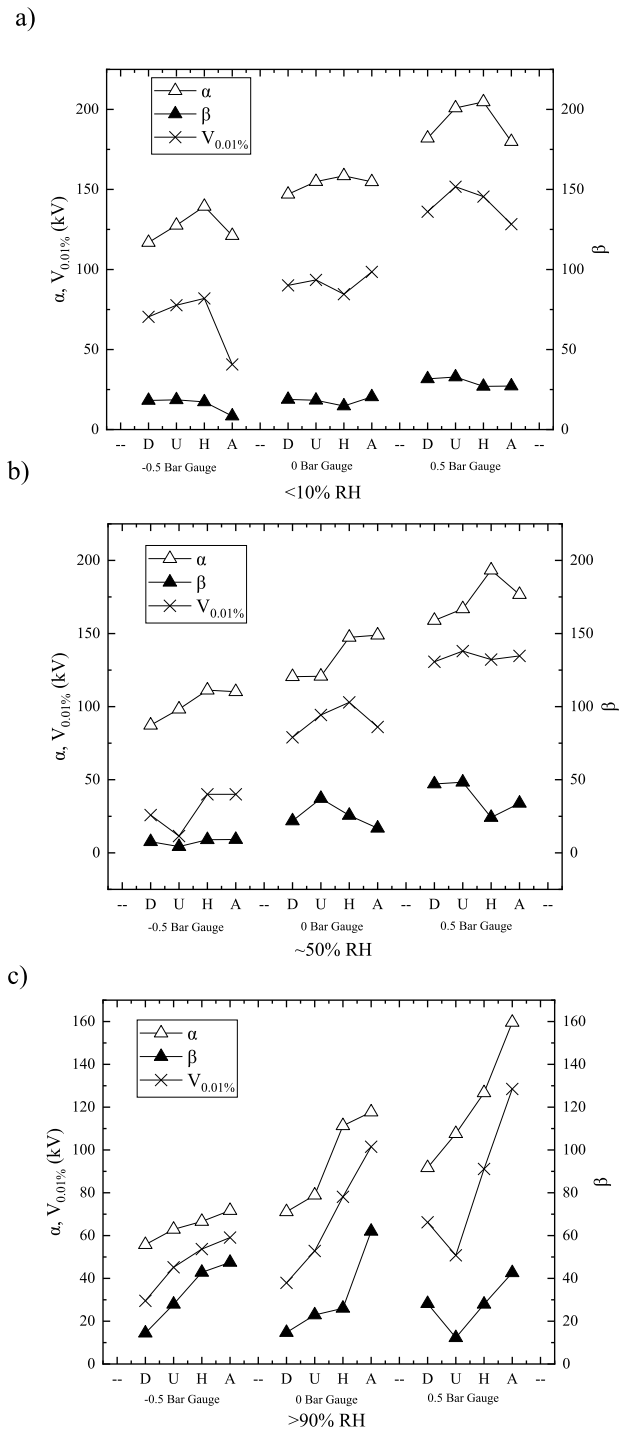


FIGURE 7. Negative-polarity scale (α), shape (β) and $V_{0.01\%}$ by spacer material: D = Delrin, U = Ultem, H = HDPE and A = Air (no spacer), at different pressures and at: a) <10% RH; b) ~50% RH; and c) >90% RH. Connecting lines are for visual guidance only.

2) POSITIVE POLARITY

This section includes the 2-parameter Weibull analysis results and discussion corresponding to the positive-polarity flashover data in Fig. 6

Shown in Figs. 8a (<10% RH), 8b (~50% RH) and 8c (>90% RH) are the 2-parameter Weibull parameters for

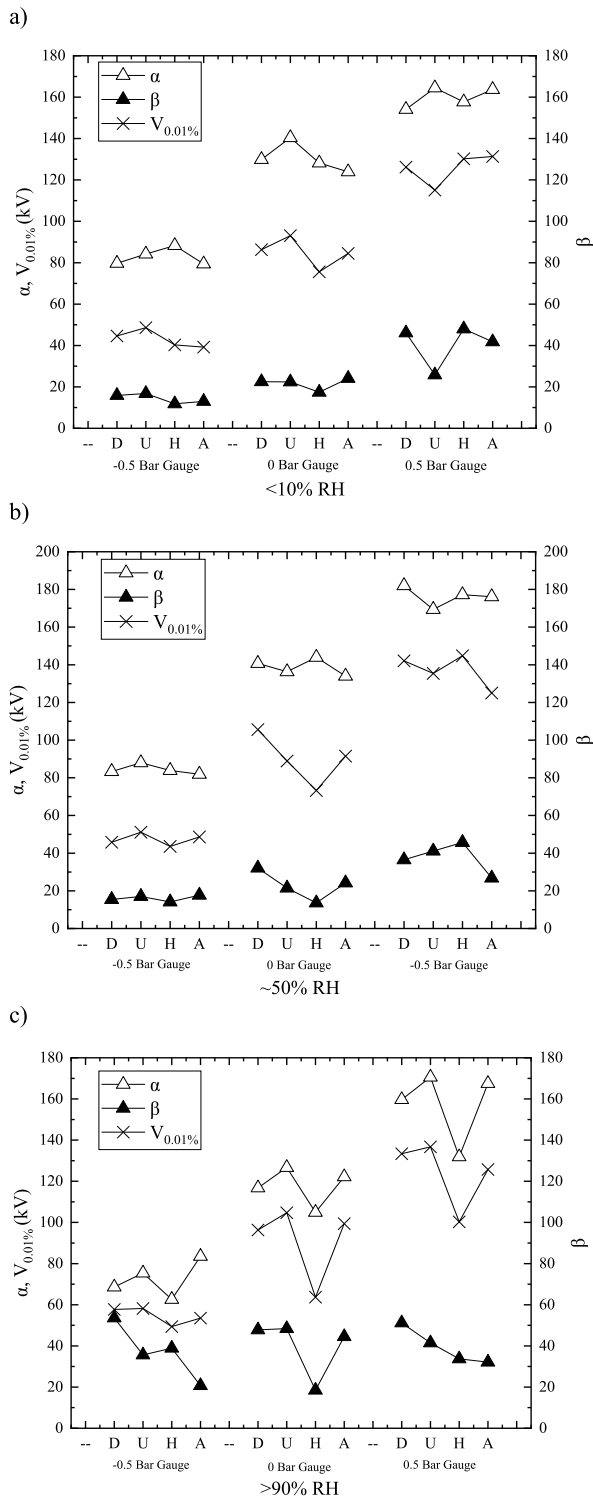


FIGURE 8. Positive-polarity scale (α), shape (β) and $V_{0.01\%}$ by spacer material: D = Delrin, U = Ultem, H = HDPE and A = Air (no spacer), at different pressures and at: a) <10% RH; b) ~50% RH; and c) >90% RH. Connecting lines are for visual guidance only.

positive polarity, for each set of test conditions. As before, the 0.01% probability value generally follows the same trend as α , with the β values determining the difference between these two points. This can be seen from Fig. 8c, where,

at -0.5 bar gauge, the elevated β value for Delrin results in a much smaller difference in values compared to that for an open air gap, where β was much lower. This then informs on the sensitivity of the system for each change. As the RH was increased, the 0.01% probability value showed a slight increase due to the general β increase when comparing values at both, <10% RH and ~50% RH, with those at >90% RH. However, as seen for negative polarity also, as the humidity is elevated to >90% RH, the trend becomes more erratic.

The 0.01% probability values are reduced in comparison to the α values the most for HDPE, at 0 bar gauge at ~50% RH, with the lower β value measured due to the increased range of breakdown voltages for these conditions. As the pressure was increased, the scale parameter, α , increased. Unlike for negative polarity, however, no dependence on the permittivity of the material was observed. In terms of β , a small increase in value is evident with increasing pressure at <10% RH and at ~50% RH, although for >90% RH there is no discernible trend.

Overall, for both negative and positive polarity, there is a general increase in α , corresponding to the increasing flashover voltages shown in section III, with increasing pressure. With increasing humidity, the same trend is seen as for the average breakdown voltage values shown in Figs. 5 and 6, where a decrease is seen for negative polarity, while α is generally a consistent value for positive polarity. Values of β were shown to generally increase as the pressure increased and as the humidity increased, although the behavior is more erratic at >90% RH, for both polarities. This indicates that the range of the breakdown values observed is decreasing as pressure increases, and as humidity increases. Values of $V_{0.01\%}$ were found to generally increase with increasing pressure, governed by the increase of α and the corresponding β values.

V. DISCUSSION

The observed results are now discussed in terms of the parameters that had a marked effect on the flashover voltage in the testing phase.

A. MATERIAL

Comparing the results by material highlights the effect that the relative permittivity of the solid spacer had on certain tests. Under negative polarity, the performance of the system was shown to follow the assumption of higher flashover strengths for lower permittivity [17], [18]. This behavior was observed for all three levels of RH and all three levels of pressure, as evident from Fig. 5. This observation is based on changes in the average flashover voltages, although, the error bars do overlap. This decrease in flashover voltage is due to the field enhancement associated with increasing relative permittivity of the spacer material, resulting in lower flashover voltages [17], [18]. Under positive polarity, however, the same effect was not observed. This is due to different breakdown processes affecting the initiation and propagation of the discharge, including higher

probability of bulk air breakdown, away from the surface of the spacer [3], [13], [19].

B. HUMIDITY

Increasing the relative humidity resulted in significant changes in the performance of the insulation systems. It was observed that, under negative polarity, increasing RH was detrimental to the system, with the flashover voltage decreasing. However, under positive polarity, the reduction in flashover voltage with increasing RH was not so substantial. Particularly between <10% RH and ~50% RH, the flashover voltage at ~50% RH was found to be either equal to, or greater than, that at <10% RH. At <10% RH, a substantial asymmetric performance of the gap was evident when changing impulse polarity. This polarity effect is due to the ratio of gap spacing to electrode diameter. With no spacer between the electrodes, the discharges were initiated from the electrode edges, where the field is increased by ~87% compared to the average field (V/d), as shown in Fig. 2. That is, the field distribution at the electrode edges can be classified as quasi-uniform, similar to that of the sphere gaps tested in [9] and [10]. In [9] and [10], it is shown that, for different ratios of gap spacing, S , to sphere diameter, D , the breakdown behaviour of a geometrically-symmetrical electrode arrangement is not always electrically symmetrical. The ratio S/D determines the mechanism of the electrical breakdown, and the resultant breakdown voltage of the system. Using the same method, S/D for the current system is calculated to be ~2. From [10], it is seen that this system falls within the 'low positive sparkover range', which results in a higher negative breakdown voltage.

In [9], the authors state that: "*In sphere spacings greater than $1.6 \sqrt{R}$ the influence of ground on the flux distribution causes higher voltage gradients to exist on the ungrounded sphere than exist on the grounded sphere at sparking distances*". This effect of higher voltage gradients resulting when one of the electrodes is grounded is supported by [20]–[22], where grounding of one electrode is shown to affect the field distribution in geometrically-symmetrical electrode setups, which can manifest in differences in the positive and negative breakdown voltages. The simulation results in Fig. 2 support this phenomenon, as the field at the HV electrode is seen to be over two times higher than that at the grounded electrode, resulting in a field distribution closer to that of a sphere-plane gap, where negative breakdown voltages are higher than positive. These differences in breakdown performance are discussed in [9]: where the electrode setup falls within the 'low positive sparkover range', the positive breakdown voltage is lower than the negative, due to electrons being absorbed by the positive HV electrode, leaving behind positive space charge in the gap. This positive space charge increases the effective ionisation zone, and adds to the HV electrode potential, leading to breakdown. For negative polarity, electrons are repelled by the HV electrode and are subject to electron attachment due to the electronegativity of

the gas, or the electrons are held by the positive space charge at the outer boundary of the ionised region.

Further work on symmetrical rod gaps is reported in [23] and [24], where differences in positive and negative breakdown voltages of up to 100 kV were also shown. In the present work, an increase of the relative humidity of the gas between the electrodes was seen to decrease the magnitude of the difference between positive and negative breakdown voltages - this is potentially due to water droplets forming on the grounded electrode of the vertically-aligned system due to gravity, and increasing the field strength, as shown in [25], potentially counteracting the asymmetrical performance caused by the S/D ratio.

In order to further understand the reasons for this behaviour with the addition of a dielectric spacer, the location of formation of the plasma channel and subsequent discharge path upon breakdown was visually inspected during testing. The plasma channel at breakdown was seen to initiate and terminate at different points in the electrode system, dependent upon the test parameters. The different test conditions resulted in three distinct flashover behaviours:

- a surface flashover, with the discharge coupled closely to the surface of the solid spacer;
- a flashover at the higher-field regions associated with the electrode edges, away from the surface of the solid spacer;
- a flashover initiated at the edge of one electrode, but terminating at a position on the opposite electrode, between the triple junction point and the rounded electrode edge.

Differences in flashover behavior were also evident when comparing spacer material. As the humidity was elevated to >90% RH, HDPE was found to have similar performance for both, positive and negative, polarity. This similar behaviour at >90% RH is thought to be due to the consistent discharge path for HDPE at each level of pressure, with discharges either all emanating from the triple junction, or all from the electrode edge, irrespective of polarity. Therefore, the system can be viewed as being symmetrical when the solid spacer is formed from HDPE. However, with Delrin and Ultem spacers, there is a clear polarity effect, correlating with observations on the discharge path changing with different polarities as the humidity increases. This polarity effect for Ultem and Delrin is thought to be due to the fact that surface flashover was generally observed under elevated RH for negative polarity, whereas bulk breakdown of the humid air at >90% RH, away from the solid surface, was generally observed for positive polarity. This behavior has been discussed in [3], [13], which show that positive impulsive discharges develop away from the surface of the insulating spacer. This was due to charge deposition from surface discharges accumulating on the surface of the solid spacer, culminating in an abundance of induced polarization charges, causing field distortions that can affect the avalanche process close to the spacer surface [19]. This can be attributed to the application of impulses that did not result in breakdown from the 'step up' process, but contributed

to an increase in surface charge. This is also seen in [26], where the surface charge has been shown to increase with the number of impulses the dielectric is subject to. In the present study, the negative-polarity breakdown voltages were found to decrease drastically at elevated ($>90\%$ RH) humidity levels. This results in a higher positive-polarity flashover voltage compared to that for negative polarity, due to the initiation and termination points of the plasma channel during flashover. This can be explained further by the following phenomena. Firstly, differences in hydrophobicity can change the way that water vapour accumulates on the surfaces of the different spacer materials. For hydrophobic materials such as HDPE, the accumulation of water droplets on the surface can result in their movement under the action of an applied electrical field. This movement of water droplets along the spacer surface eliminates the high-field regions that would otherwise be created by the accumulation of droplets at the triple junction, increasing the flashover initiation voltage and, thus, the breakdown voltage [27]–[29]. This is particularly evident for negative polarity, where the discharge is more likely to propagate over the surface of materials at higher levels of RH [3], [13].

Under positive polarity, the discharges propagate through the bulk air with Delrin and Ultem spacers, resulting in the flashover voltage being lower for negative polarity. As the humidity increases to $>90\%$ RH, water accumulates on the spacer surfaces, creating a more conductive surface over the length of the solid dielectric [30]. Therefore, the resistivity associated with the air-solid interface will decrease, and the flashover voltage will decrease accordingly, as seen from the test results in Figs. 5 and 6.

Overall, the effect of RH on the flashover voltage can be discussed in the context of the results in Fig. 5 (negative polarity). With no solid spacer ('air'), the discharge is initiated from the high-field region at the electrode edges. Comparing the results at $>90\%$ RH, there is a clear reduction in the average flashover voltage of the gap when bridged by a solid (HDPE, Delrin and Ultem) spacer, which can be correlated with an increased tendency for the discharge to propagate closer to the material surface. The effect is lesser for HDPE due to the hydrophobicity of the material, which increases the surface flashover voltage, as previously discussed. This behaviour can also be seen for positive polarity (Figs. 6a and 6b), where the flashover voltage of the open air gap is similar to that with Delrin and Ultem spacers, corresponding to the propagation of the discharge through the bulk air during these tests. For HDPE, however, flashover is initiated at much lower voltages, suggesting a discharge path close to the surface of the solid. This was confirmed by visual inspection during testing. The tendency for matching discharge processes between negative and positive polarity breakdown with HDPE under high humidity results in the symmetrical performance at $>90\%$ RH for HDPE, as shown in Figs. 5 and 6. The maximum difference between negative- and positive-polarity breakdown voltages over the three pressures tested is 7 kV, at 0 bar gauge. When comparing this

to Ultem and Delrin at $>90\%$ RH, the maximum difference between polarities is 65 kV and 68 kV, respectively, both at 0.5 bar gauge.

The presence of water molecules at higher levels of RH also increases the attachment coefficient of the air, due to the electronegative nature of the water molecules [31]. At higher pressures, the flashover voltages could be higher at $\sim 50\%$ RH, due to the attachment coefficient increasing compared to that at $<10\%$ RH. Further increase of the humidity to $>90\%$ RH, however, will lead to a decrease in breakdown voltage from that at $\sim 50\%$ RH, due to water droplets formed on the electrodes at $>90\%$ RH, creating high-field regions and decreasing the average breakdown voltage, as the disruptive discharge voltage becomes irregular [32]. It has also been shown, in [33], that the rate of increase of the attachment coefficient is considerably greater than that of the ionisation coefficient, as the partial pressure of water vapour is increased. In addition, the secondary ionisation coefficient was found to decrease with increasing water-vapour pressure [34]. In consequence, an increase in applied voltage is required to attain the same ionisation efficiency and affect breakdown.

C. POLARITY

As discussed in sections III and V-B, a polarity effect was evident throughout testing. To reiterate, this polarity effect can be attributed to the ratio of gap spacing to electrode diameter, S/D , of the system [9], when discharges propagated between the electrode edges. The discharge path is also a potential reason for the differences between positive- and negative-polarity breakdown voltages, as the increase of humidity alters the discharge location when a dielectric spacer bridges the electrodes. It is known that streamers generally propagate away from the spacer material under positive applied voltages [3], [13], an effect that was also observed visually during the testing phase herein. This behaviour was evident for specific sets of environmental conditions, at $\sim 50\%$ RH and $>90\%$ RH, where the potential increase of the conductivity in the vicinity of the surface of the added dielectric spacer could alter the spark path, compared to that observed at lower levels of RH. However, at $<10\%$ RH, the lack of moisture introduced into the system created an asymmetric performance between positive and negative polarity, due to the asymmetric field distribution shown in Fig. 2. This resulted in the differences in breakdown voltage being statistically significant to one standard deviation, as the discharge always initiated at the high-field regions of the system (electrode edges), leading to a higher negative polarity breakdown voltage. As the humidity is increased, negative streamers generally propagate along the surface of spacer materials, compared to the bulk breakdown of air observed for positive streamers, resulting in differences in flashover voltage. This can be clearly seen in Figs. 5 and 6, where the positive-polarity flashover voltages at $>90\%$ RH are higher than those for negative polarity, for Delrin and Ultem spacers. Another difference between positive and

negative polarity is that, for positive polarity, the flashover voltage generally increased with increasing humidity, particularly from <10% RH to ~50% RH. Whereas, for negative polarity, the flashover voltages decreased with increasing RH. This can be attributed to the fact that humidity inhibits the inception and development of positive impulsive discharges, but exerts minimal influence upon negative streamers [35].

Overall, the influence of RH on the breakdown voltage can be explained by the following phenomena. For positive polarity, the increase in breakdown voltage with increasing RH could be due to the lesser amount of space charge generated under positive polarity at high humidity. There is experimental evidence, [36]–[38], that supports the notion that positive space charge diminishes with increasing humidity. Results reported in [39] also show a difference in corona inception voltages, with negative inception voltages being lower than positive, due to the effect of humidity.

D. OPEN GAP ANALYSIS

Comparing the breakdown voltages measured without solid spacers only, some interesting effects were observed with changing RH. For negative polarity, increased humidity was found to decrease the flashover strength of the air gap. Particularly at >90% RH, the disruptive discharge voltage becomes irregular [32], due to the high-field regions caused by water droplets forming on the electrodes [25], manifested in a decrease in the breakdown voltage from 115 kV to 70 kV at <10% RH and >90% RH, respectively, at –0.5 bar. However, for positive polarity, the effect of increasing humidity was minimal throughout the tests, with average flashover voltages of 75 kV at <10% RH, and 80 kV at >90% RH, at –0.5 bar gauge pressure. This effect was also seen in [40], where no change in breakdown voltage was found for lightning impulses for humid air, with moisture content ranging from 300 ppm to 1500 ppm. The results found here generally follow what was found in [41], [42], where there was a general breakdown voltage increase of 5%–10% with increasing moisture content. This could be due to photoionisation processes, which are important in the positive-streamer breakdown mechanism, where high-energy photons are absorbed by water molecules at high levels of relative humidity [33], requiring an increase in applied voltage to cause breakdown.

Reinforcement of breakdown strength due to the humidity can be observed when the relative humidity is higher than ~60%–90%. For positive polarity, the open air gap breakdown voltage is seen to remain consistent for all levels of RH. At –0.5 bar gauge, the breakdown voltage is seen to slightly increase with increasing relative humidity. This was also seen in [1], where the average breakdown voltage of an air gap was found to increase slightly with increasing humidity, from 9.8 g/m³ to 20.7 g/m³. Also, in [4], [12], the effect of very high levels of humidity on the breakdown strength were reported, where above 80% RH, the breakdown voltages were unpredictable in amplitude. For all tested conditions, increasing the pressure resulted in increased flashover voltage, as expected. As the gas pressure increases, the electron mean

free path decreases, and the collision frequency increases. Electrons will gain less energy between collisions, which means that a higher applied field is required for free electrons to gain sufficient energy in order to cause an ionisation event [34].

VI. CONCLUSION

In this paper, the effect of reduced (<10% RH), medium (~50% RH) and elevated (>90% RH) levels of humidity on the flashover strength of gas-solid gaps, and of open gaps, has been investigated. Experimental results for flashover in air at pressures around atmospheric pressure, and for impulse voltages of both polarities, have been reported, and the mechanisms associated with flashover for the different sets of test conditions have been discussed herein. It is important for designers of insulation systems to note that, dependent upon specific system characteristics (ratio of gap spacing to electrode diameter), an asymmetrical electrical performance can result, even for a geometrically-symmetrical electrode arrangement. This information is imperative in the design process of any pulsed power system, where it is critical to understand the variation in the values of failure voltages evident under different applied voltage regimes or operational conditions. From the results and associated statistical analysis, it can be concluded that the introduction of moisture typically decreases the flashover strength at very high (>90% RH) levels of humidity, for negative polarity test conditions. However, at ‘medium’ levels (~50% RH) of humidity, there is a similar operational performance, if not better, for a composite gas-solid insulation system, compared to an open gas gap, under certain circumstances, due to the electronegative effect of humid air. The location of the discharge path is very important in highlighting the mechanisms involved in the flashover process and the associated flashover voltage, with the ratio of S/D introducing an obvious effect in a symmetrical, parallel-plane, electrode geometry.

The highest achieved flashover voltage of ~200 kV was with an HDPE spacer in <10% RH air, under negative polarity impulses and at 0.5 bar gauge. The lowest breakdown voltage of ~53 kV throughout the testing was for Delrin, for negative polarity, and at –0.5 bar gauge and >90% RH.

Further work will include measuring the flashover voltage of the insulation system with solid spacers with modified (‘knurled’) surface finishes, in attempts to improve the performance of these spacers under the same experimental conditions, without increasing the inter-electrode distance.

ACKNOWLEDGEMENT

The authors would also like to acknowledge Andy Carlin, Sean Doak, and Louis Cooper from the HVT Workshop, Department of Electronic and Electrical Engineering, University of Strathclyde, for their assistance with the manufacturing process.

REFERENCES

- [1] L. Lazaridis and P. Mikropoulos, “Positive impulse flashover along smooth cylindrical insulating surfaces under variable humidity,” *IEEE Trans. Dielectr. Electr. Insul.*, vol. 18, no. 3, pp. 745–754, Jun. 2011.

- [2] J. T. Krile, A. A. Neuber, J. C. Dickens, and H. G. Krompholz, "DC flashover of a dielectric surface in atmospheric conditions," *IEEE Trans. Plasma Sci.*, vol. 32, no. 5, pp. 1828–1834, Oct. 2004.
- [3] L. Gao, "Comparison of long sparks in air and over an insulator surface," in *Proc. 11th Int. Symp. High-Voltage Eng. (ISH)*, London, U.K., 1999, pp. 31–34.
- [4] H. Niu and T. Xu, "The relevance between dramatic declines of air gap breakdown voltage and fog-haze weather," in *Proc. IEEE Region Conf. (TENCON)*, Nov. 2015, pp. 1–4.
- [5] T. S. Sudarshan and R. A. Dougal, "Mechanisms of surface flashover along solid dielectrics in compressed gases: A review," *IEEE Trans. Electr. Insul.*, vol. EI-21, no. 5, pp. 727–746, Oct. 1986.
- [6] Accessed: Oct. 15, 2020. [Online]. Available: <https://plastim.co.uk/wp-content/uploads/2019/07/HDPE-PE-300-Technical-Data-Sheet.pdf>
- [7] *Utem Data Sheet*. Accessed: Oct. 15, 2020. [Online]. Available: <https://www.plasticstockist.com/downloads/datasheets/pei1000.pdf>
- [8] *Delrin Data Sheet*. Accessed: Oct. 15, 2020. [Online]. Available: https://www.theplasticshop.co.uk/plastic_technical_data_sheets/delrin_acetal_homopolymer_technical_data_sheet.pdf
- [9] F. O. Mcmillan and E. C. Starr, "The influence of polarity on high-voltage discharges," *Trans. Amer. Inst. Electr. Eng.*, vol. 50, no. 1, pp. 23–33, Mar. 1931, doi: [10.1109/T-AIEE.1931.5055733](https://doi.org/10.1109/T-AIEE.1931.5055733).
- [10] F. O. Mcmillan, "Polarity limits of the sphere gap," *Trans. Amer. Inst. Electr. Eng.*, vol. 58, no. 2, pp. 56–61, Feb. 1939, doi: [10.1109/T-AIEE.1939.5057923](https://doi.org/10.1109/T-AIEE.1939.5057923).
- [11] ASTM International *Standard Test Method for Dielectric Breakdown Voltage and Dielectric Strength of Solid Electrical Insulating Materials Using Impulse Waves*, Standard D3426-97, ASTM International, West Conshohocken, PA, USA, 1997, doi: [10.1520/D3426-97](https://doi.org/10.1520/D3426-97).
- [12] H. Niu, R. Guo, T. Xu, and J. Xu, "Research on weather condition of significant decline of air gap breakdown voltage," in *Proc. IEEE 15th Int. Conf. Environ. Electr. Eng. (EEEIC)*, Rome, Italy, Jun. 2015, pp. 1725–1729.
- [13] L. A. Lazaridis, P. N. Mikropoulos, A. Darras, and A. Theocharis, "Flashover along cylindrical insulating surfaces under positive lightning impulse voltages," in *Proc. 17th Int. Conf. Gas Discharges Appl.*, Wales, U.K., 2008, pp. 233–236.
- [14] M. Wilson, S. Macgregor, M. Given, I. Timoshkin, M. A. Sinclair, K. J. Thomas, and J. Lehr, "Surface flashover of oil-immersed dielectric materials in uniform and non-uniform fields," *IEEE Trans. Dielectr. Electr. Insul.*, vol. 16, no. 4, pp. 1028–1036, Aug. 2009.
- [15] *Guide for the Statistical Analysis of Electrical Insulation Breakdown Data*, International Standard IEC 62539(E): 2007 (IEEE Standard 930-2004), Jul. 2007.
- [16] W. Weibull, "Statistical distribution function of wide applicability," *Trans. ASME J. Appl. Mech.*, vol. 18, no. 3, pp. 293–297, 1951.
- [17] N. Matsuoka, Y. Fuchi, M. Kozako, and M. Hikita, "Effect of permittivity variation on surface flashover of GIS epoxy spacer model in SF₆ gas," in *Proc. IEEE Int. Conf. Dielectr. (ICD)*, Montpellier, France, Jul. 2016, pp. 96–99.
- [18] D. L. Schweickart, H. Kirkici, L. C. Walko, and W. G. Dunbar, "Insulation and dielectric breakdown design considerations in sub-atmospheric environments," in *Proc. 16th IEEE Int. Pulsed Power Conf.*, Albuquerque, NM, USA, Jun. 2007, pp. 1661–1664.
- [19] I. Gallimberti, G. Marchesi, and L. Niemeyer, "Streamer corona at an insulator surface," in *Proc. 7th Int. Symp. HV Eng.*, Dresden, Germany, 1991, Paper 41.10.
- [20] R. Arora and W. Mosch, *High Voltage and Electrical Insulation Engineering*. Hoboken, NJ, USA: Wiley, sec. 2, p. 19.
- [21] A. L. Maglaras, L. A. Maglaras, and V. F. Topalis, "The influence of the effect of grounding and corona current on the field strength the corona onset and the breakdown Voltage of Small Air Gaps," *WSEAS Trans. Power*, vol. 3, no. 1, pp. 103–108, Jan. 2008.
- [22] Z. Qiu and J. Ruan *Electric Field Features and Its Application for Air Gap Breakdown Voltage Prediction*, M. Shekholeslami, Ed. London, U.K.: InTechOpen, 2018, pp. 187–209.
- [23] A. Carrus, E. Cinieri, A. Fumi, and C. Mazzetti, "Short tail lightning impulse behaviour of medium voltage line insulation," *IEEE Trans. Power Del.*, vol. 14, no. 1, pp. 218–226, Jan. 1999, doi: [10.1109/61.736725](https://doi.org/10.1109/61.736725).
- [24] E. Kuffel and M. Abdullah, "Corona and breakdown-voltage characteristics in sphere—Plane and rod—Rod gaps under impulse voltages of various wavefront durations," *Proc. Inst. Electr. Eng.*, vol. 113, no. 6, pp. 1113–1119, Jun. 1966, doi: [10.1049/piee.1966.0182](https://doi.org/10.1049/piee.1966.0182).
- [25] Z. Guan, L. Wang, B. Yang, X. Liang, and Z. Li, "Electric field analysis of water drop corona," *IEEE Trans. Power Del.*, vol. 20, no. 2, pp. 964–969, Apr. 2005, doi: [10.1109/TPWRD.2004.837672](https://doi.org/10.1109/TPWRD.2004.837672).
- [26] J. Deng, S. Matsuoka, A. Kumada, and K. Hidaka, "The influence of residual charge on surface discharge propagation," *J. Phys. D, Appl. Phys.*, vol. 43, no. 49, 2010, Art. no. 495203.
- [27] W. Pfeiffer and K. Ermeler, "Influence of humidity exposure time on dielectric properties of insulation material surfaces," in *Proc. Annu. Rep. Conf. Electr. Insul. Dielectric Phenomena*, Austin, TX, USA, vol. 2, 1999, pp. 492–495.
- [28] A. Krivda and D. Birtwhistle, "Breakdown between water drops on wet polymer surfaces," in *Proc. Annu. Rep. Conf. Electr. Insul. Dielectric Phenomena*, Kitchener, ON, Canada, 2001, pp. 572–580.
- [29] B. Kumar Gautam, Y. Mizuno, G. Matsubayashi, K. Sakanishi, T. Kawaguchi, and R. Matsuoka, "Effect of wetting conditions on the contamination flashover voltages of polymer insulators," in *Proc. IEEE 8th Int. Conf. Properties Appl. Dielectric Mater.*, Bali, Indonesia, Jun. 2006, pp. 538–541.
- [30] R. K. Raiput, *A Textbook PF Electrical Engineering Materials*, vol. 171. Laxmi Publications Pvt Limited, 2004.
- [31] E. Kuffel, "Influence of humidity on the breakdown voltage of sphere-gaps and uniform-field gaps," in *Proc. IEE A, Power Eng.*, vol. 108, no. 40, pp. 295–301, Aug. 1961.
- [32] *High-Voltage Test Techniques—Part 1: General Definitions and Test Requirements*, document EN 60060-1:2010.
- [33] E. Kuffel, "Electron attachment coefficients in oxygen, dry air, humid air and water vapour," *Proc. Phys. Soc.*, vol. 74, p. 297, Sep. 1959.
- [34] L. G. Christophorou and L. A. Pinnaduwa, "Basic physics of gaseous dielectrics," *IEEE Trans. Electr. Insul.*, vol. 25, no. 1, pp. 55–74, Feb. 1990.
- [35] D. E. Gourgoulis, P. N. Mikropoulos, C. A. Stassinopoulos, and C. G. Yakinthos, "Effects of negative DC pre-stressing on positive impulse breakdown characteristics of conductor-rod gaps," *IEE Proc. Sci., Meas. Technol.*, vol. 152, no. 4, pp. 155–160, Jul. 2005.
- [36] A. J. Davies, J. Dutton, R. Turri, and R. T. Waters, "The effect of humidity on space charge growth in short air gaps," in *Proc. 5th Int. Symp. Gaseous Dielectr.*, Knoxville, TN, USA, vol. 58, 1987, pp. 249–254.
- [37] N. L. Allen and G. Dring, "Effect of humidity on the properties of corona in a rod—Plane gap under positive impulse voltages," *Proc. R. Soc. Lond. A, Math. Phys. Eng. Sci.*, vol. 396, no. 1811, pp. 281–295, 1984.
- [38] L. R. Group, "Positive discharges in long air gaps," *Electra*, vol. 53, p. 97, 1977.
- [39] T. Kondo, R. Ozaki, and K. Kadowaki, "Effect of superposed repetitive pulses onto DC voltage on discharge extension into fog water produced by electrospray," in *Proc. Int. Symp. Electr. Insulating Mater. (ISEIM)*, Toyohashi, Japan, Sep. 2017, pp. 390–393.
- [40] J.-K. Seong, W.-J. Shin, J.-S. Hwang, J.-G. Lee, B.-W. Lee, K.-B. Seo, and D.-H. Jeong, "Effect of humidity and electrode roughness on the AC and impulse breakdown characteristics of dry-air," in *Proc. IEEE Int. Conf. Condition Monitor. Diagnosis*, Sep. 2012, pp. 770–773.
- [41] A. Davies and R. Turri, "Effect of humidity and gas density on switching impulse breakdown of short airgaps," *Phys. Sci.*, vol. 135, pp. 59–68, Jan. 1988.
- [42] D. Rodriguez, R. Gorur, and P. Hansen, "Effect of humidity on the breakdown characteristics of air in uniform field for the very low frequency (VLF) band," *IEEE Trans. Dielectr. Electr. Insul.*, vol. 16, no. 5, pp. 1397–1403, Oct. 2009, doi: [10.1109/TDEI.2009.5293953](https://doi.org/10.1109/TDEI.2009.5293953).



RUAIRIDH W. MACPHERSON (Graduate Student Member, IEEE) was born in Inverness, Scotland, in 1990. He received the B.Eng. (Hons.) and M.Phil. degrees from the University of Strathclyde, in 2016 and 2019, respectively, where he is currently pursuing the Ph.D. degree with the High Voltage Technologies Group, Department of Electronic and Electrical Engineering. His research interests include work in corona-stabilised switches, with particular focus on environmentally friendly gas dielectrics and surface flashover of gas-solid interfaces within sub-optimal environmental conditions.



MARK P. WILSON (Member, IEEE) was born in Stranraer, Scotland, in 1982. He received the B.Eng. (Hons.), M.Phil., and Ph.D. degrees in electronic and electrical engineering from the University of Strathclyde, Glasgow, U.K., in 2004, 2007, and 2011, respectively. He is currently with the High Voltage Technologies Research Group, University of Strathclyde. His research interests include interfacial surface flashover, nanodielectrics, the practical applications of high power ultrasound, corona discharges, and pulsed electric fields. He is a member of the IEEE Nuclear and Plasma Sciences Society, from whom he received a Graduate Scholarship Award in 2011, the IEEE Dielectrics and Electrical Insulation Society, and the IET.



IGOR V. TIMOSHKIN (Senior Member, IEEE) received the degree in physics from Moscow State University, Moscow, Russia, in 1992, and the Ph.D. degree from the Imperial College of Science, Technology and Medicine (ICSTM), London, U.K., in 2001. He was a Researcher with Moscow State Agro-Engineering University, Moscow, and then with the Institute for High Temperatures of Russian Academy of Sciences, Moscow. In 1997, he joined ICSTM. Then, he joined the Department of Electronic and Electrical Engineering, University of Strathclyde, Glasgow, U.K., in 2001, where he became a Reader in 2016. His research interests include dielectric materials, pulsed power, transient spark discharges, and environmental applications of non-thermal plasma discharges. He is currently a Voting Member of the Pulsed Power Science and Technology Committee in the IEEE Nuclear and Plasma Science Society, a member of International Advisory Committee of the IEEE Conference on Dielectric Liquids, a member of the International Scientific Committee of the Gas Discharges and Their Application Conference, and a Subject Editor of *IET Nanodielectrics*.



SCOTT J. MACGREGOR (Senior Member, IEEE) received the B.Sc. and Ph.D. degrees from the University of Strathclyde, Glasgow, U.K., in 1982 and 1986, respectively. He became a Pulsed Power Research Fellow in 1986 and a Lecturer in pulsed-power technology in 1989. In 1994, he became a Senior Lecturer, with a promotion to a Reader and a Professor of High Voltage Engineering, in 1999 and 2001, respectively. In 2006 and 2010, he became the Head of the Department of Electronic and Electrical Engineering and the Executive Dean of the Faculty of Engineering. He has been the Vice-Principal of the University of Strathclyde since 2014. He was a recipient of the 2013 IEEE Peter Haas Award, and he was appointed as an Associate Editor of the IEEE TRANSACTIONS ON DIELECTRICS AND ELECTRICAL INSULATION in 2015. His research interests include high-voltage pulse generation, high-frequency diagnostics, high-power repetitive switching, high-speed switching, electronic methods for food pasteurization and sterilization, generation of high-power ultrasound (HPU), plasma channel drilling, pulsed-plasma cleaning of pipes, and stimulation of oil wells with HPU.



MARTIN J. GIVEN (Senior Member, IEEE) received the degree in physics from the University of Sussex in 1981 and the Ph.D. degree in electronic and electrical engineering from the University of Strathclyde in 1996. He is currently a Senior Lecturer with the Department of Electronic and Electrical Engineering, University of Strathclyde. His research interests include ageing processes and condition monitoring in solid and liquid insulation systems, high-speed switching and pulse power applications, fundamental study of plasma sources, and fabrication of micro- or nanostructured surfaces.

...